



Implementation and non-intrusive characterization of a hybrid active–passive liner with grazing flow

Benjamin Betgen^{a,1}, Marie-Annick Galland^a, Estelle Piot^{b,*}, Frank Simon^b

^a Centre Acoustique du Laboratoire de Mécanique des Fluides et d'Acoustique (LMFA), Ecole Centrale de Lyon, 69134 Ecully Cedex, France

^b Onera – The French Aerospace Lab, F31055 Toulouse, France

ARTICLE INFO

Article history:

Received 17 June 2011

Received in revised form 19 January 2012

Accepted 31 January 2012

Available online 25 February 2012

Keywords:

Duct acoustic

Flow

Acoustic liner

Impedance control

LDV

ABSTRACT

Different hybrid active–passive absorbers have been developed at the LMFA that seem well suited for the use as turboengine nacelle liners. The basic version is made of a resistive screen backed by cells that contain one microphone and one secondary source each. At low frequencies, acoustic pressure behind the screen is cancelled actively in order to obtain a purely real and constant surface impedance. At higher frequencies, active control is turned off and the liner acts as a classical SDOF resonator. An advanced version (the complex hybrid absorber) has been developed recently, featuring two microphones per cell. With the new system, the surface impedance of the cell can be measured and adjusted to a given (possibly complex and frequency dependent) target impedance. The present paper reports on two measurement campaigns that aimed at a characterization of these absorbers by the use of Laser Doppler Velocimetry (LDV). LDV allows the assessment of acoustic velocity in vicinity of the absorber in a non intrusive way. The measurements confirm the good performance of both absorbers without flow. In particular, one observes that in active mode the different hybrid cells appear as a homogeneous liner with a global influence on the duct. In presence of grazing flow, the influence of the absorber on the duct is limited to the immediate vicinity of each hybrid cell, which explains the reduced performance.

© 2012 Elsevier Ltd. All rights reserved.

1. Introduction

Passive acoustic treatments like single-degree-of-freedom (SDOF) liners are widely used in aeroengine nacelle inlets and outlets for the reduction of turbofan noise. They are typically made of a thin resistive sheet above a honeycomb layer, and are designed to behave as 1/4-wavelength resonators [1]. Then, the thicker the liner, the lower the frequency range of sound attenuation. However, as available space inside nacelles is limited, it is generally impossible to tune such SDOF resonators to the low blade-passing-frequencies (BPF) of modern high-bypass-ratio engines, or to adapt them to different flight conditions. Purely active noise control techniques on the other hand are limited to the low frequency range. Hybrid active–passive liners allow these limitations to be overcome and assure good performance over a broad frequency range [2]. The general design of a hybrid cell is depicted in Fig. 1. It is made of a resistive screen above a cavity backed by a secondary source. At high frequencies, this source is turned off and the hybrid liner acts as classical SDOF resonators. At low frequencies, active noise control techniques are used in order to adapt the surface impedance of the liner. In this paper two control

techniques are presented. The first one can be summarized as “impedance control through pressure control”. Indeed, pressure is cancelled on the rear side of the resistive screen, which results in a purely real surface impedance, given by the resistance of the used screen [3,4]. This kind of hybrid liner is herein denoted as *basic hybrid absorber*. However the optimal impedance (i.e. the one that produces the highest noise reduction) of an absorber for flow duct applications is generally a frequency-dependent complex number, that is why a second control technique is proposed: it consists in performing a full impedance control by using one microphone on each side of the screen. Such a liner is denoted as *complex hybrid absorber*. The first concept has been introduced in 1953 by Olson and May [5], who suggested performing a pressure reduction at the rear face of a porous layer in order to enhance absorption at low frequencies. Many other devices have then been proposed to realize active systems able to control, partially or totally, the impedance. Among recent publications, electrical circuits have been designed to directly control the impedance of the secondary source: Kanev and Mironov [6] present a device able to adapt the impedance of a mechanical resonator, with a unique microphone, in order to enhance absorption for a plane wave under normal incidence. Lissek et al. [7] propose a theory unifying all the passive and active acoustic impedance control strategies, introducing the concept of electroacoustic absorbers. A potential application is the design of active devices without any external

* Corresponding author. Tel.: +33 5 62 25 28 12; fax: +33 5 62 25 25 83.

E-mail address: estelle.piot@onera.fr (E. Piot).

¹ Present address: VibraTec, 28 chemin du petit bois, 69131 Ecully Cedex, France.

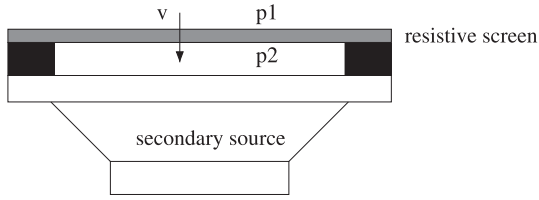


Fig. 1. Principal setup of a hybrid cell.

sensor. The control techniques used in the present paper are detailed in Section 2.

These hybrid liners, and especially the complex hybrid absorber, have been shown to be very efficient noise attenuators since transmission loss values up to 20 dB can be obtained in a duct without flow [8].

But the application as aeroengine nacelle liner would implicate grazing flow of relatively high Mach number. Due to a more complex control algorithm and the added front face microphone, flow induced noise can be critical for the complex hybrid absorber. In contrast, the error microphones of the basic hybrid absorber are well protected against grazing flow behind the resistive layer; fast convergence and excellent stability have been observed [9], even in the presence of high flow-induced noise levels. However, for both kind of active control, the measured transmission loss decreases clearly with increasing flow speed [8].

In order to better understand this loss of performance with flow, the present study aims at a local observation of the sound field in vicinity of the absorber. Laser Doppler Velocimetry (LDV) offers the opportunity of such a local and non-intrusive determination of acoustic parameters. The measurements that are presented in this paper have been conducted at the French Aerospace Lab ONERA at Toulouse, and some of this work has been presented in [10]. The LDV measurement technique developed at ONERA and the corresponding aeroacoustic test bench are briefly described in Section 4.

The results of a first measurement campaign devoted to the basic hybrid absorber are given in Section 5.1. The complex hybrid absorber has been tested during a second campaign that is discussed in Section 5.2.

2. The hybrid liner

2.1. Impedance control through pressure control: the basic hybrid absorber

At low frequencies, viscous forces in a porous material predominate over inertial ones and the acoustic velocity across a resistive layer can be approximated using Darcy's law. This means that acoustic velocity is proportional to the pressure difference between both sides of the resistive layer and inversely proportional to its flow resistance R , as given by Eq. (1).

$$v = \frac{p_1 - p_2}{R} \tag{1}$$

Hence, when acoustic pressure on the rear side of the layer is cancelled ($p_2 = 0$), the surface impedance is given by the flow resistance R according to Eq. (2).

$$Z = \frac{p_1}{v} = R \tag{2}$$

Pressure cancellation can be obtained by backing the resistive layer with a cavity of depth $\lambda/4$. The use of active control allows the realization of the same boundary condition at low frequencies without the need of a deep cavity. In addition, the $p_2 = 0$ condition can then be obtained over a broad frequency range. This is the

principle of what is qualified as hybrid absorber in previous publications [3,9,4]. Throughout the present paper it will be labeled *basic hybrid absorber* in order to distinguish this absorber from the newly developed version.

Fig. 3a displays the basic hybrid absorber used during the first measurement campaign. A surface of 30 mm × 150 mm is imposed by the sample holder of the ONERA test bench. Miniature loudspeakers (Monacor SP-5) have been selected as secondary sources. Those exceed the width of the liner sample holder, therefore the cavities of the hybrid cells are chosen deep enough (40 mm) to fix the loudspeakers outside the sample holder.

The control system that performs the pressure minimization is a digital feedback controller. Indeed, for industrial applications it is necessary to consider a liner made of a large number of hybrid cells. However, with a classical Multiple Input Multiple Output

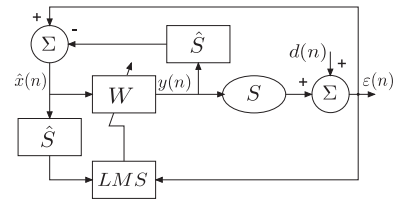
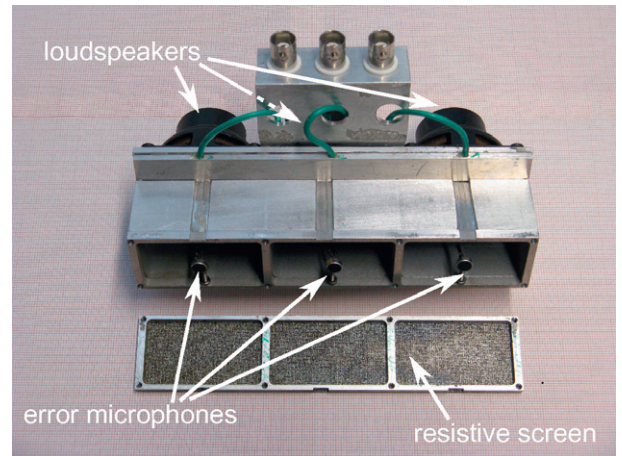
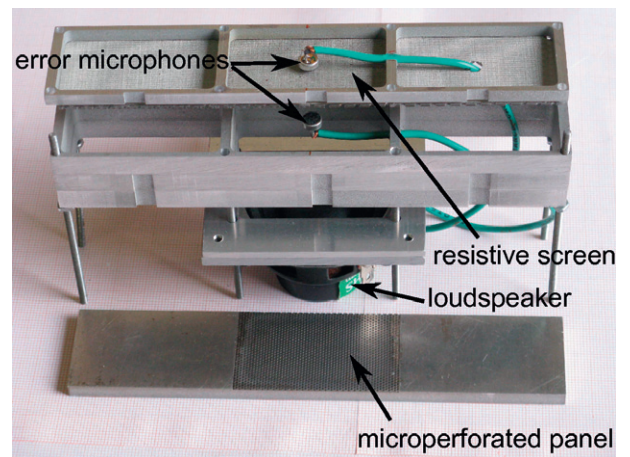


Fig. 2. Block diagram of the IMC-FXLMS algorithm.



(a) 3-cell basic hybrid absorber



(b) 1-cell complex hybrid absorber

Fig. 3. Hybrid absorber prototypes.

(MIMO) feedforward system based on a unique reference signal, memory and calculation costs significantly increase with the number of channels. Moreover, in flow duct applications, an upstream reference signal may be insufficiently correlated with the sound to be cancelled downstream, and could then prevent from achieving an efficient active control. Thus, a digital adaptive feedback control system has been developed [4], which operates independently cell by cell. The SISO (Single Input Single Output) version

of the algorithm consists in removing the feedback contribution coming from the secondary source, from the signal obtained at the control microphone. The primary contribution only remains and is then used as a reference signal in the classical FXLMS algorithm. The corresponding block diagram of this algorithm called IMC-FXLMS algorithm for Internal Model Control is shown in Fig. 2. S represents the secondary path, between the secondary source and the control microphone. \hat{S} is a estimate of S realized

Table 1

Optimal impedances predicted by the numerical model for a liner of 50 mm width and 150 mm length in a tube of cross-section 50 mm × 50 mm (Z_{num}), compared to Cremer impedance (Z_{Cremer}).

Frequency (Hz)		496	992	1592
$M = 0$	$Z_{num}/\rho C_0$	0.1 – 0.11i	0.21 – 0.21i	0.34 – 0.37i
	$Z_{Cremer}/\rho C_0$	0.13 – 0.01i	0.27 – 0.02i	0.42 – 0.04i
$M = 0.1$	$Z_{num}/\rho C_0$	0.1 + 0.03i	0.2 – 0.07i	0.33 – 0.23i
	$Z_{Cremer}/\rho C_0$	0.11 – 0.01i	0.22 – 0.02i	0.35 – 0.03i

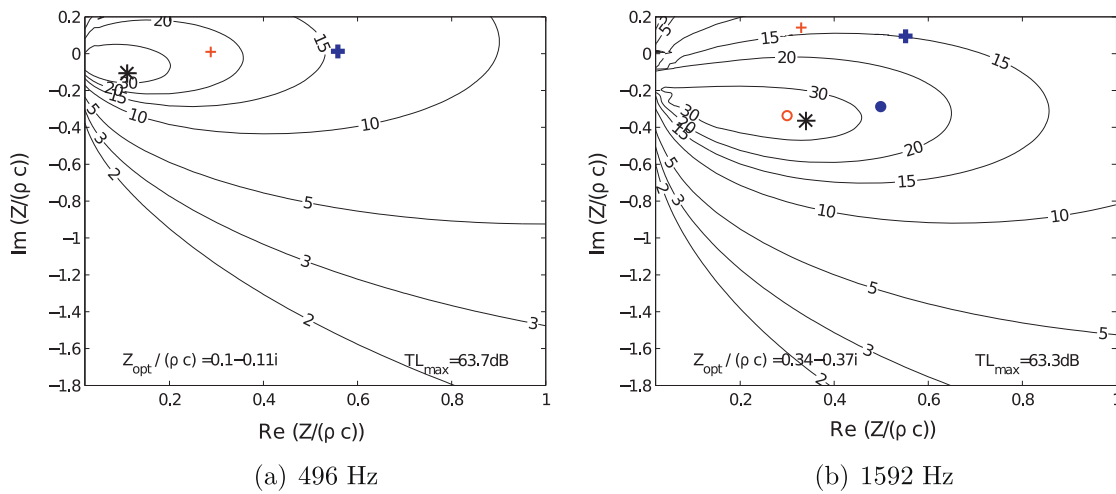


Fig. 4. Transmission loss as a function of complex impedance of a liner of 50 mm width and 150 mm length in a tube of cross-section 50 mm × 50 mm. No flow. Comparison between $f = 496$ Hz and $f = 1592$ Hz. The optimal impedance is marked with a star. Impedances realized with two different resistive screens of the basic hybrid absorber are given by crosses in the basic active mode and circles in the passive mode (thin, open: feltmetal sheet; thick, closed: wiremesh sheet). At 496 Hz the passive mode impedance is outside the figure.

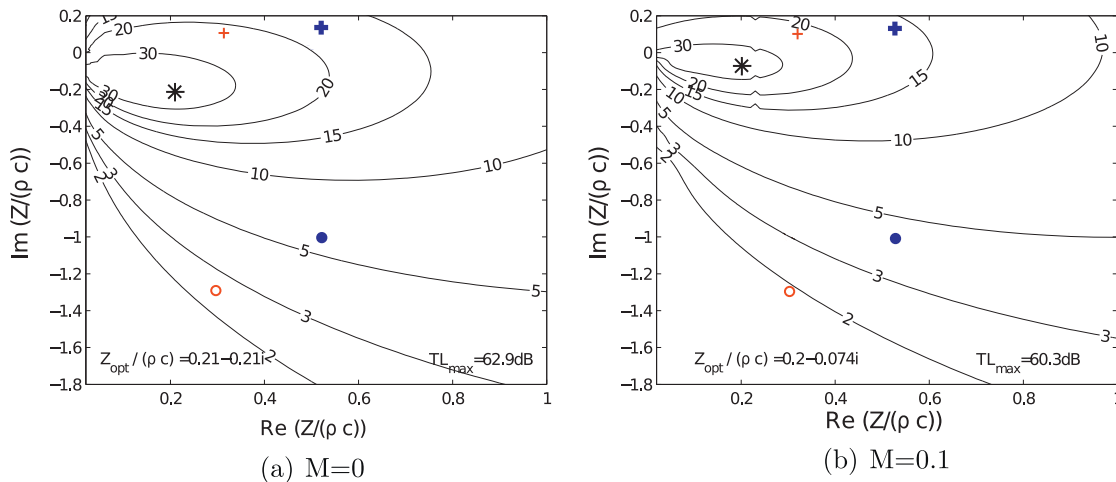


Fig. 5. Transmission loss as a function of complex impedance of a liner of 50 mm width and 150 mm length in a tube of cross-section 50 mm × 50 mm. Frequency $f = 992$ Hz. Comparison between $M = 0$ and $M = 0.1$. The optimal impedance is marked with a star. Impedances realized with two different resistive screens of the basic hybrid absorber are given by crosses in the basic active mode and circles in the passive mode (thin, open: feltmetal sheet; thick, closed: wiremesh sheet).

by a numerical FIR filter, predetermined before control. W is the adaptive control filter. $d(n)$ is the primary disturbance, $\hat{x}(n)$ its estimate and thus the synthesized reference for the FXLMS algorithm. $y(n)$ is the controller output, and $\varepsilon(n)$ is the error signal, measured at the control microphone. More information about this algorithm can be found in Refs. [3,11].

Error microphones are electret condenser microphones Panasonic WM65. Two different resistive screens are used: a feltmetal sheet of resistance $R/\rho c_0 = 0.3$ and a wiremesh glued on a perforated panel of $R/\rho c_0 = 0.5$. Both materials are thin layers (around 1 mm) that are suitable for use under harsh environmental conditions.

2.2. Full impedance control: the complex hybrid absorber

Making use of Eq. (1), the surface impedance of the hybrid absorber can be written as

$$Z = \frac{p_1}{v} = R \frac{p_1}{p_1 - p_2} \tag{3}$$

It becomes clear that arbitrary surface impedances can be obtained by rearranging p_1 and p_2 instead of only cancelling p_2 . The velocity measurement according to Eq. (1) has the advantage of being frequency independent (in the low frequency range).

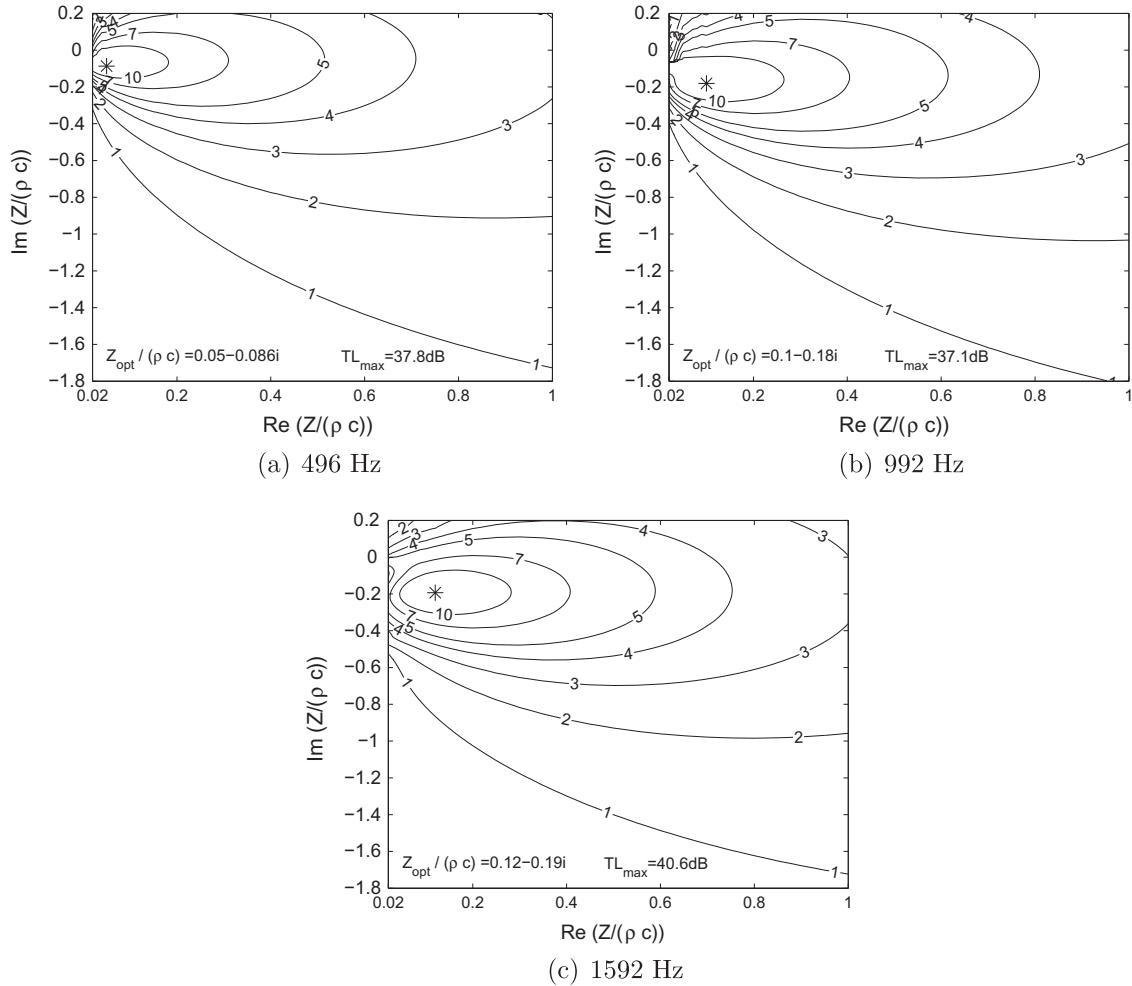


Fig. 6. Transmission loss as a function of complex impedance of a liner of 50 mm width and 50 mm length in a tube of cross-section 50 mm × 50 mm. $M = 0$.

Table 2

Numerical optimum and measured values of impedances and associated TL for different modes of operation of the complex hybrid absorber, without flow.

Frequency (Hz)		496	992	1592
Numerical optimum	$Z/\rho c_0$	0.05 – 0.086i	0.1 – 0.18i	0.12 – 0.19i
	TL (dB)	37.8	37.1	40.6
Passive mode	$Z/\rho c_0$	0.40 – 2.00i	0.43 – 0.77i	0.49 – 0.13i
	TL (dB)	0.0	1.5	4.3
Basic active mode	$Z/\rho c_0$	0.56 + 0.11i	0.58 + 0.22i	0.62 + 0.35i
	TL (dB)	2.6	2.1	3.0
Active impedance ctrl. mode	$Z/\rho c_0$	0.01 – 0.14i	0.11 – 0.18i	0.27 – 0.15i
	TL (dB)	22.3	14.0	7.2

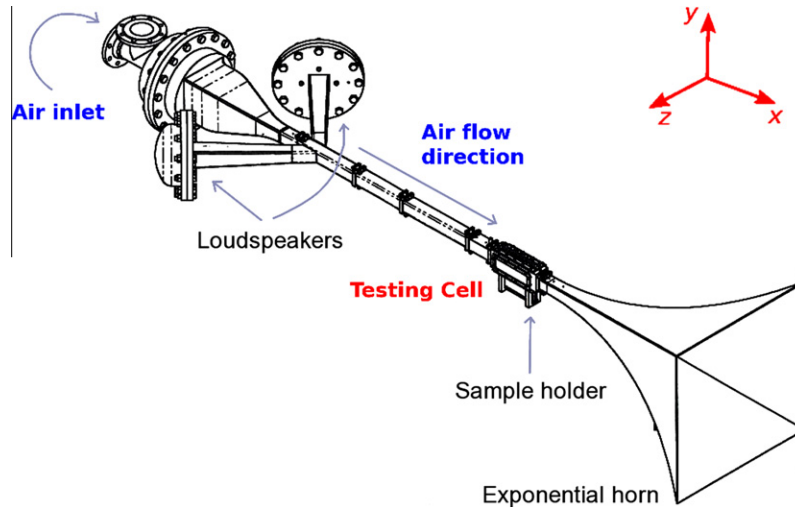


Fig. 7. Sketch of the Aero-Thermo-Acoustic test bench.

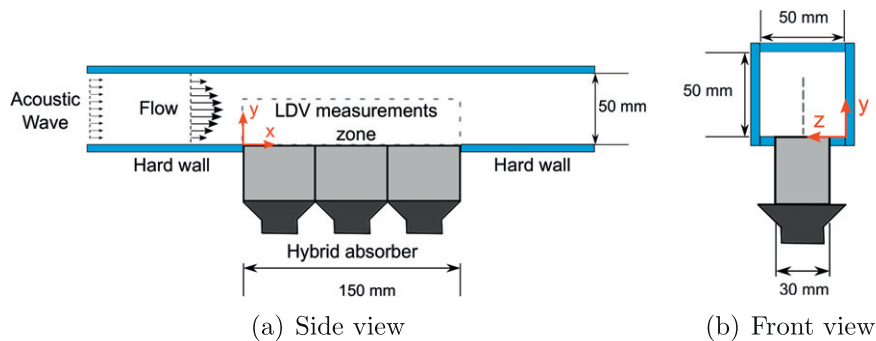


Fig. 8. Sketch of the test section equipped with the hybrid liner. For the complex hybrid absorber, only the central cell is used.

Additionally, no large distance between the microphones is needed because the pressure gradient is provided by the resistive screen. Surprisingly, this apparently self-evident expression has – to our knowledge – never been used for impedance control applications. Introducing a target impedance Z_t , Eq. (3) can directly be rewritten as an error signal.

$$\epsilon = Z_t(p_1 - p_2) - Rp_1 \quad (4)$$

As complex impedances can be realized by the use of this error signal, the new hybrid absorber is qualified as *complex hybrid absorber*. The error signal is integrated in a digital feedback control structure similar to the one mentioned above. Therefore, the target impedance, usually defined in the frequency domain has to be expressed in the time domain to build a numerical error signal; details can be found in Ref. [8]. At this stage, only a one channel version of the complex hybrid absorber has been realized as displayed in Fig. 3b. A Monacor SP-5 speaker is again used as secondary source, the resistive layer is the wiremesh screen of $R/\rho c_0 = 0.5$. The pair of Panasonic WM65 microphones has been verified to respect maximum errors in magnitude and phase of 1 dB and 12° respectively. Fig. 3b also shows a microperforated panel at the front face of the device: it is used in order to protect the front face microphone measuring the p_1 pressure from flow. Of course, the impedance modification due to the layer and the added distance has to be taken into account when defining the target impedance.

3. Optimal impedance

This section aims at illustrating the benefit of impedance control in contrast to conventional absorbers.

3.1. Theory

It is well known that the optimal impedance for absorption of a normal incident plane wave would be $Z_0 = \rho c_0$. This is not the case for grazing incidence. Cremer [12] found an analytic expression for the optimal impedance of a treatment covering one face of an infinitely long rectangular duct. This optimal impedance given by $Z_{Cremer} = Z_0(0.91 - 0.76j)kh/\pi$ only depends on frequency and the height of the duct (perpendicular to the liner). Tester [13] gives a correctional factor of $1/(1+M)^2$ to account for the presence of uniform flow of Mach number M in the direction of sound propagation.

In the case of an infinitely long liner the optimal impedance is simply the one that produces the highest absorption. For a liner of finite length, optimal impedance is better defined as the one producing the highest transmission loss² (TL), since noise attenuation can be produced by both reflection of the incoming acoustic wave and absorption of it. An analytical expression of the optimal

² The classical definition of the best liner is the one that produces the highest insertion loss. However, in the duct configuration considered here, the insertion loss is equal to the transmission loss.

impedance may be difficult to find, but its value can easily be determined numerically. However, the qualitative behavior of optimal impedance is common to the infinite as well as to the finite liner: the real part is positive and increasing with frequency, the imaginary part is negative and decreasing. Transmission loss produced by a very short liner can to a great extent be due to reflection, this is the reason why the optimal impedance of a short liner is generally much lower in modulus than the Cremer impedance. Furthermore, mean flow in the direction of sound propagation also lowers the optimal impedance; in the opposite direction optimal impedance is increased. In this context it must be pointed out that the presented experiments always deal with flow in the direction of sound propagation. A setup with flow in the opposite direction would be advantageous for absorption but is not available in the present work.

Transmission loss of a finite length liner is determined numerically. As all considered frequencies remain below the cut-off frequency of the duct, a harmonic plane wave source and an anechoic termination are assumed. The acoustic pressure field within the duct is estimated by a multimodal expansion model, similar to that used in [14–16] and validated against literature results [17]. The simulated duct is divided into three zones with diverse boundary conditions along their walls. The first zone corresponds to the incident region; the duct walls are entirely rigid, and the source is modeled as an incident plane wave. The second zone is the treated region. A uniform impedance boundary condition is imposed on one

of the walls, and the classical displacement continuity relation [18] is used when a uniform mean flow is taken into account. The complex modes in this section are determined by using an iterative algorithm. The last zone corresponds to a rigid wall duct with an anechoic termination. The respective modal amplitudes are determined in each region by applying pressure and velocity continuity relations at each interface. All details can be found in Ref. [19]. Transmission loss is defined as the logarithmic ratio between the power incident towards the treated region and the power transmitted through the treated region. As only plane waves are considered and as a reflection free termination assumption is made, the TL equals to the logarithmic ratio between the amplitude of the incident pressure wave in the first zone and the amplitude of the transmitted pressure wave in the last zone. This TL is calculated by varying both real part and imaginary part of the impedance, leading to the determination of the optimal impedance.

3.2. Results in the configuration of the basic hybrid absorber

Let us now consider the example of calculated optimal impedances for a liner of 50 mm width and 150 mm length in a tube of section 50 mm × 50 mm. While the dimensions of the tube correspond to the ONERA test duct, the dimensions of the liner do not exactly equal the basic hybrid liner (which is 30 mm wide and 150 mm long). In fact, the consideration of a liner that does not cover the entire duct width would substantially complicate

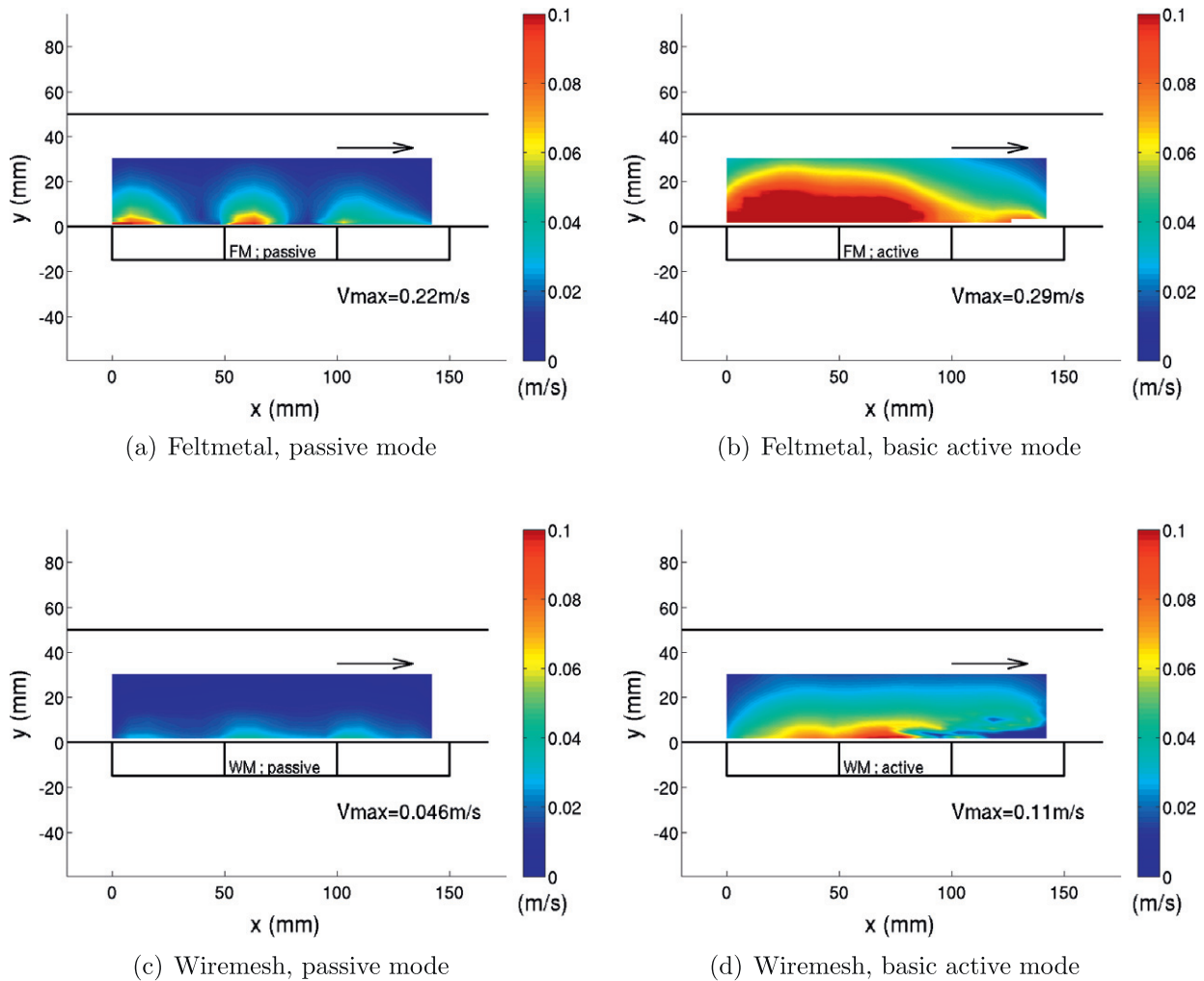


Fig. 9. Acoustic velocity in y-direction at 496 Hz, hybrid cell, $M = 0$.

the determination of its optimal impedance. The calculations presented here will therefore only serve as a qualitative comparison between the feltmetal and the wiremesh screen. Different results are summed up in Table 1, and compared to Cremer impedance of the same tube. In the case with a uniform flow, the Cremer impedance is modified according to Tester [13].

Fig. 4 represents curves of equal TL in the complex impedance plane at two different frequencies. In the case of the basic hybrid absorber, the real part of the surface impedance is independent of frequency and is given by the resistance of the layer, its choice is therefore of high importance. The imaginary part of the surface impedance is controlled by the pressure cancellation on the rear side of the layer in basic active mode, while it is fixed by the geometrical features of the absorber in passive mode. Four impedances are marked in particular, representing the two different resistive screens in basic active and passive mode. These impedances have been measured in a standing wave tube, without flow. Basic active control mainly changes the reactance, which becomes approximately zero at low frequencies. At higher frequencies, Eq. (1) is not valid anymore and the reactance is slightly positive. In passive mode, the reactance is essentially that of the cavity, which can be expressed as $-1/\tan kL$, where k is the frequency-dependent wavenumber and L the depth of the cavity. As the cavity is about 40 mm deep, the reactance is around -2.6 at 496 Hz, this value being outside of the figure.

Fig. 4a makes clear that at low frequencies basic active control leads to an impedance close to the optimal one. At the same time, the resistive layer of lower resistance outperforms the one with higher resistance. At higher frequency (see Fig. 4b at 1592 Hz), the close-to-zero reactance obtained in the basic active mode is far from the optimal one, and consequently the passive mode is supposed to produce a higher transmission loss than the basic active mode.

Fig. 5 gives the curves of equal TL at 992 Hz for the cases without flow and for a uniform mean flow of $M = 0.1$. The impedances of the basic hybrid liner measured in the standing wave tube for the two different resistive screens in basic active and passive mode are also plotted. The same value of impedances are used with and without flow. The presence of uniform flow slightly moves the position of the optimal impedance. The expected performance of both materials, however, is not dramatically changed. For instance, the predicted TL value for the basic hybrid absorber with a wiremesh sheet in basic active mode is of 17.1 dB without flow and 15.8 dB with a $M = 0.1$ flow.

In summary, the presented predictions show that the fixed resistance of the basic hybrid absorber represents a tradeoff between low and high frequency performance. The utility of an absorber which is capable of realizing arbitrary complex impedances at different frequencies is therefore evident, that is why the complex hybrid absorber is considered.

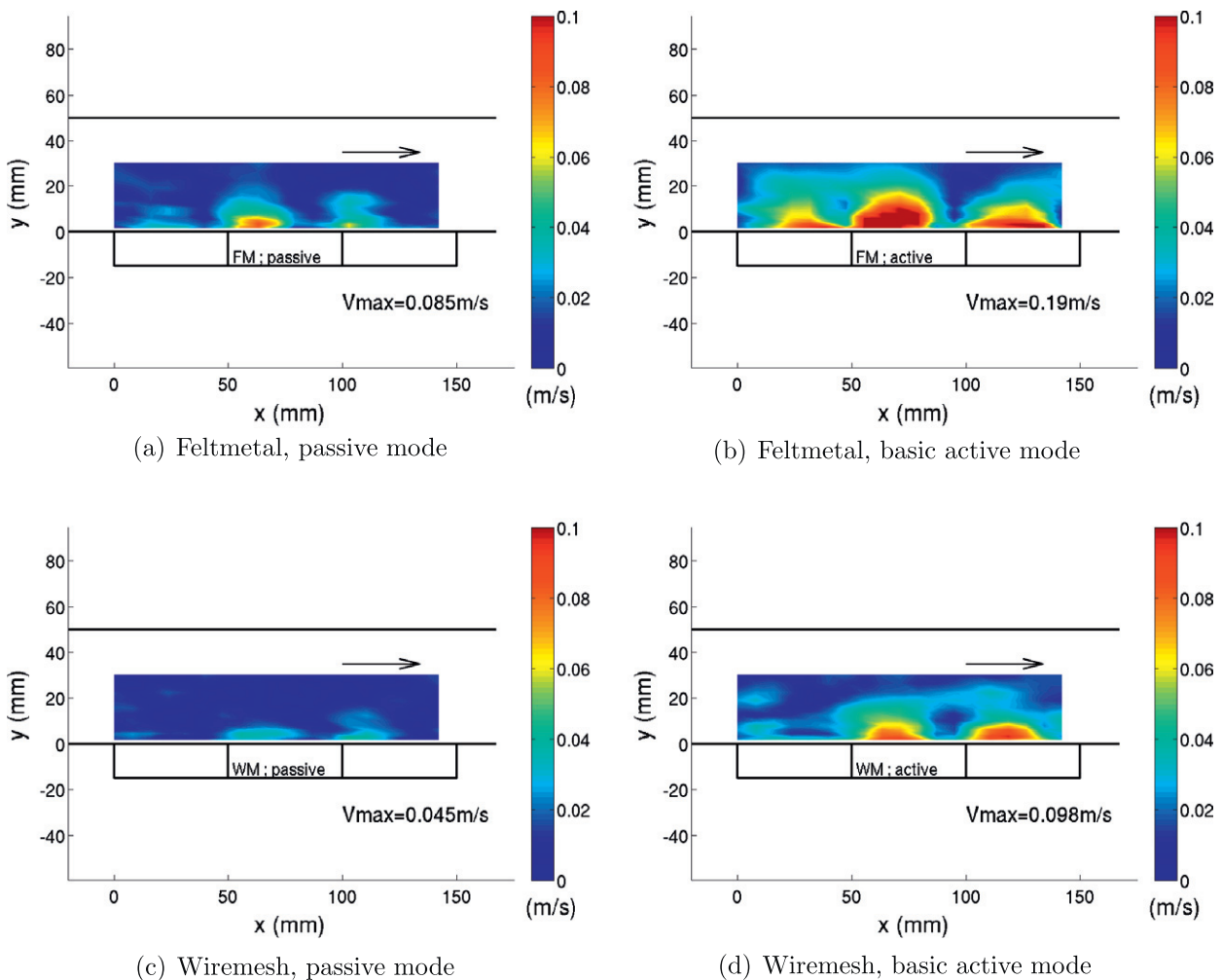


Fig. 10. Acoustic velocity in y-direction at 496 Hz, hybrid cell, $M = 0.1$.

3.3. Results in the configuration of the complex hybrid absorber

As the developed complex hybrid absorber is shorter than the basic hybrid absorber, Figs. 4 and 5 cannot be used for the prediction of TL. Fig. 6 gives the TL-charts corresponding to this shorter absorber (length of 50 mm instead of 150 mm), the width of the absorber being still fixed at 50 mm. As the regions around the optimal impedances show extremely steep gradients, the target impedances have to be determined accurately. In order to overcome the inaccuracy of the numerical prediction due to the simplified geometry, the optimal target impedance has been determined experimentally. Table 2 indicates the numerical optimum impedance and the corresponding TL, as well as the experimental impedances measured in a standing wave tube and the corresponding TL measured in the ONERA bench. All impedances are obtained using the complex hybrid absorber in different modes of operation, i.e. passive, “basic active” (i.e. $p_2 = 0$) and “active impedance control”. In respect to the basic hybrid absorber, the impedances in “passive” and “basic active mode” are altered due to the presence of the microperforated panel above the upper microphone and the change in the distance between the top layer and the secondary source, which slightly decreases the realized resistance and increases the realized reactance. The settings in “active impedance control mode” are determined empirically by successively maximizing the measured TL. Comparison with the numerical optimum shows that they represent an impedance close to the best value, on contrary to what is obtained in the “basic active mode”.

4. LDV measurements

In order to investigate the impact of the hybrid liners on the acoustic field, Laser Doppler Velocimetry measurements have been performed. They allow a non-intrusive assessment of the acoustic field above the hybrid liner whatever the testing conditions. Some basics about the measurement of acoustic parameters by means of LDV are given in this section. More details about the used technique and the test bench at ONERA can be found in Ref. [20].

4.1. Aeroacoustic test bench at ONERA

The aeroacoustic test bench at ONERA Toulouse is made of a stainless steel tube of Section 50 mm × 50 mm; its total length is of about 4 m (see Fig. 7). The termination is equipped with an anechoic outlet. Excitation is provided by two loudspeakers installed in pressurized cabinets. Temperature can be adjusted up to 300 °C, however, the present tests are conducted at ambient temperature. Experiments are effected without grazing flow and with a grazing flow of bulk Mach number 0.1. This corresponds to a maximum speed in the center of the duct of about $M = 0.16$.

Let us define x as the axial coordinate and (y,z) as the coordinates normal to the axis. The test section shown in Fig. 8 has a silica window of 200 mm × 60 mm on each side (i.e. at $z = 0$ mm and $z = 50$ mm), the lower (i.e. $y = 0$) part is equipped with the hybrid liner. The dimension of the sample is limited to 30 mm × 150 mm, which does not cover the entire width of the duct as it has already

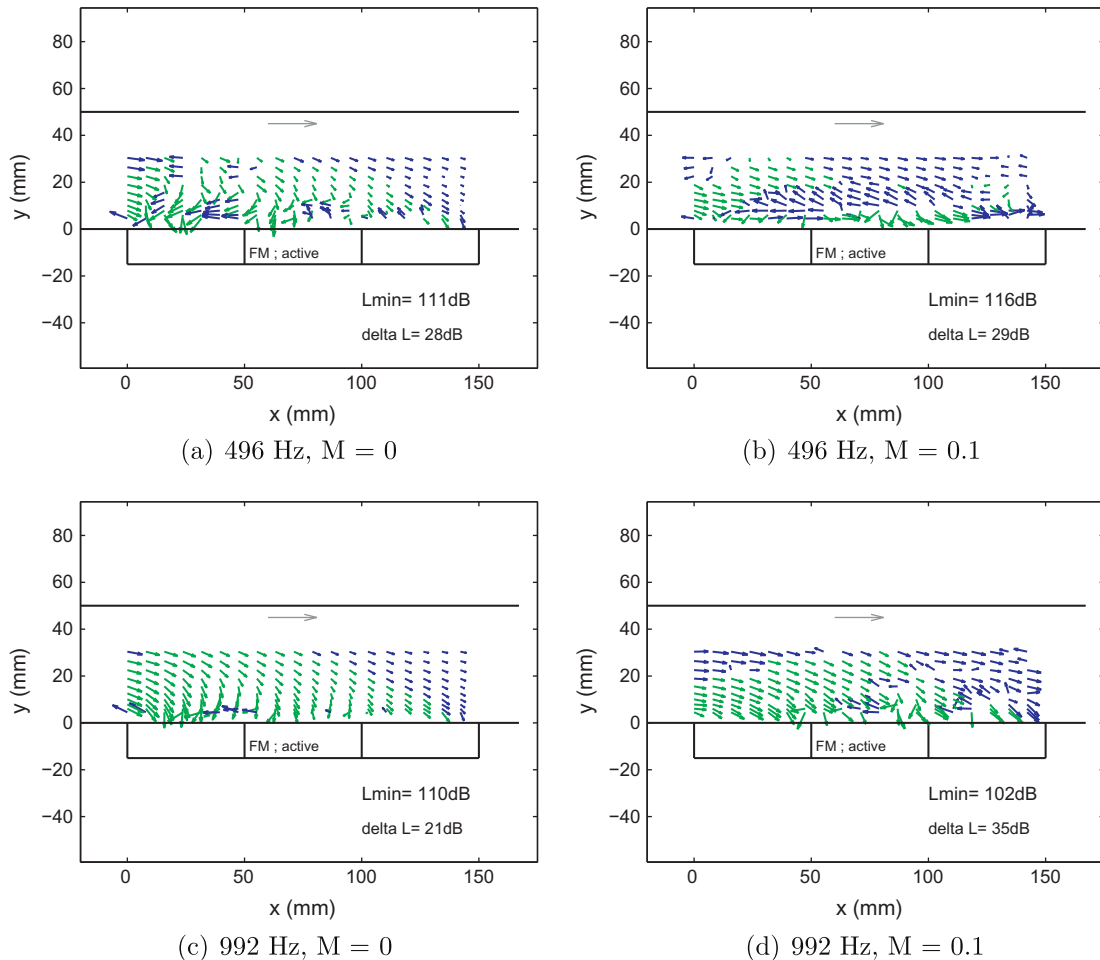


Fig. 11. Acoustic intensity at 496 Hz and 992 Hz for the feltmetal-case without and with flow, hybrid cell in basic active mode.

been mentioned. For the characterization of passive liners, the excitation signal is made of thirteen pure tones, at third octave frequencies between 312 Hz and 3136 Hz, with an overall sound pressure level of 140 dB. In active mode, the excitation is limited to three pure tones of 496 Hz, 992 Hz, and 1592 Hz. SPL of each peak is about 120 dB. At this level, the error microphones in the hybrid liner begin to saturate, which is actually unproblematic for pressure minimization. Active impedance control, however, requires a linear behavior, therefore the excitation level is decreased to about 110 dB per peak.

4.2. Data extraction and data processing

A two-components fringe mode Laser Doppler Velocimeter allows the measurement of the longitudinal (x) and normal (y) velocity components in almost the entire volume of the test section. For the present tests, only the plane $z = 25$ mm has been scanned. In order to quicken the measurements, not the entire plane is scanned but only till $y = 30$ mm. A LDV system has the particularity to provide an unevenly sampled signal due to the random arrival of particles (incense smoke) in the measurement volume. A reconstruction method is used to re-sample the raw data at a constant rate. Data processing is performed by a TSI IFA 755 system. The emitting optics produces a $100 \mu\text{m}$ -diameter measurement volume. A minimum sampling data rate of $f_m = 13,000$ measurements per second is generally ensured, for each velocity component. Each

velocity component v_x and v_y is measured by the LDV system at a given spatial location. The acoustic velocity (defined here as the component of the signal that is correlated with the excitation signal) can be deduced from the extraneous noise by a technique similar to the three-microphone signal enhancement technique [21,22]. It consists in calculating the cross-spectral density function $G_{v_i,ls}$ between the velocity signal v_i and the loudspeaker signal ls . The auto-spectral density function of the acoustic velocity reads as

$$G_{v_i} = \frac{|G_{v_i,ls}|^2}{G_{ls}} \quad (5)$$

where G_{ls} is the auto-spectral density function of the excitation signal. The acoustic velocity in the frequency domain is then given by Minotti and co-workers [23,24]

$$v'_i = \sqrt{G_{v_i}} \exp[i\Phi(v_i/ls)] \quad (6)$$

where the phase of the acoustic velocity, referenced by the excitation, is defined as

$$\Phi(v_i/ls) = \arctan \frac{\Im(G_{v_i,ls})}{\Re(G_{v_i,ls})} \quad (7)$$

Finally, acoustic pressure and acoustic intensity are deduced from the acoustic velocity field thanks to a mixed Eulerian-Lagrangian propagation model [25]. The lagrangian acoustic

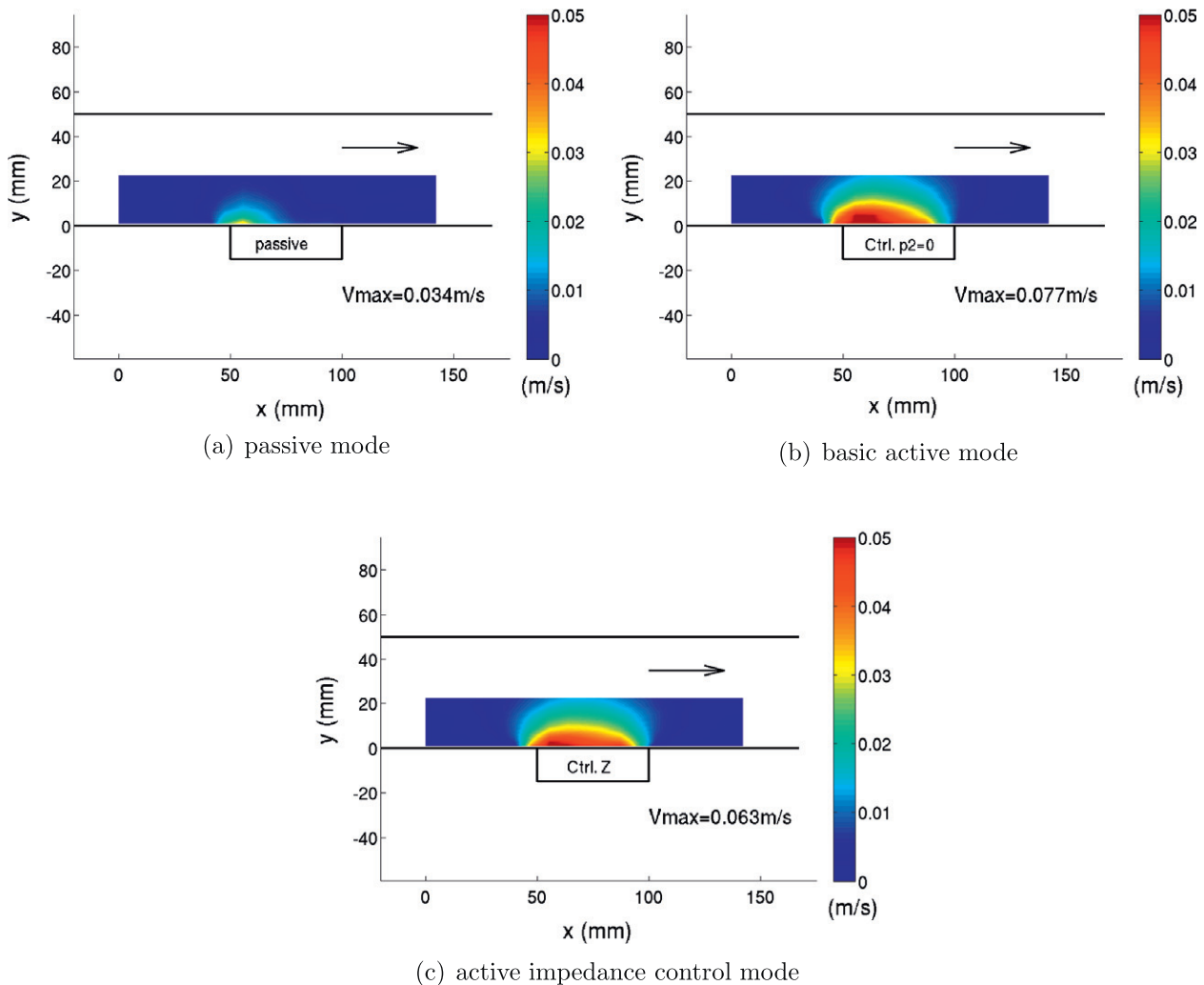


Fig. 12. Acoustic velocity in y -direction at 496 Hz, complex hybrid cell, $M = 0$.

displacement field $\vec{\xi} = (\xi_x, \xi_y)$ is obtained from the acoustic velocity field $\vec{v} = (v'_x, v'_y)$ by solving with a finite difference method the following equations:

$$U_0 \frac{\partial \xi_x}{\partial x} + i\omega \xi_x = v'_x + \frac{\partial U_0}{\partial y} \xi_y \quad (8)$$

$$U_0 \frac{\partial \xi_y}{\partial x} + i\omega \xi_y = v'_y \quad (9)$$

where U_0 denotes the mean (i.e. stationary) velocity component in the x direction (the other components are neglected). Then, the acoustic pressure reads [25]:

$$p' = -\rho_0 c_0^2 \operatorname{div} \vec{\xi} - \frac{dp_0}{dx} \xi_x \quad (10)$$

where ρ_0 , p_0 and c_0 are the density, static pressure and speed of sound of the mean flow. Finally, the active part of the acoustic intensity vector is expressed from the acoustic velocity, pressure and displacement [25]:

$$\vec{I} = \frac{1}{2} \operatorname{Re} \left[i\omega p' \vec{\xi} + i\omega \rho_0 \vec{\xi} \cdot \left(\vec{v} + \nabla U_0 \cdot \vec{\xi} \right)^* \vec{U}_0 \right] \quad (11)$$

where Re stands for the real part and $*$ is the complex conjugate. On contrary to the classical Euler formulation and the associated Cantrell and Hart intensity [26], this model yields an exact acoustic energy balance even in the presence of flow.

In comparison to pressure measurements using microphones, this approach has the advantage of being entirely non-intrusive

and of providing a complete description of the sound field in the whole measurement domain.

5. Experimental results

Both absorbers have been tested in the ONERA bench, with or without grazing flow, in order to assess their influence on the acoustic field and to understand why their efficiency is greatly reduced with flow.

5.1. The basic hybrid absorber

A first evaluation of the liner performance can be obtained on the basis of the velocity v_y normal to the liner. In a hard walled duct without flow, normal velocity would be zero in the whole duct section since only plane waves have been excited. A soft wall involves non-zero normal velocity, which leads to dissipation of energy inside the liner. Figs. 9 and 10 represent this normal velocity at 496 Hz in the $z = 25$ mm plane without flow and at $M = 0.1$ respectively. Acoustic propagation and mean flow go from the left to the right. The lowest frequency is chosen because the difference between passive and active mode is maximum here. In fact, the behavior for increasing frequencies is very much as predicted, i.e. increasing performance in passive mode and decreasing performance in basic active mode. We therefore focus on the comparison between the two different resistive layers on the one hand and on the influence of flow on the other hand for a fixed frequency.

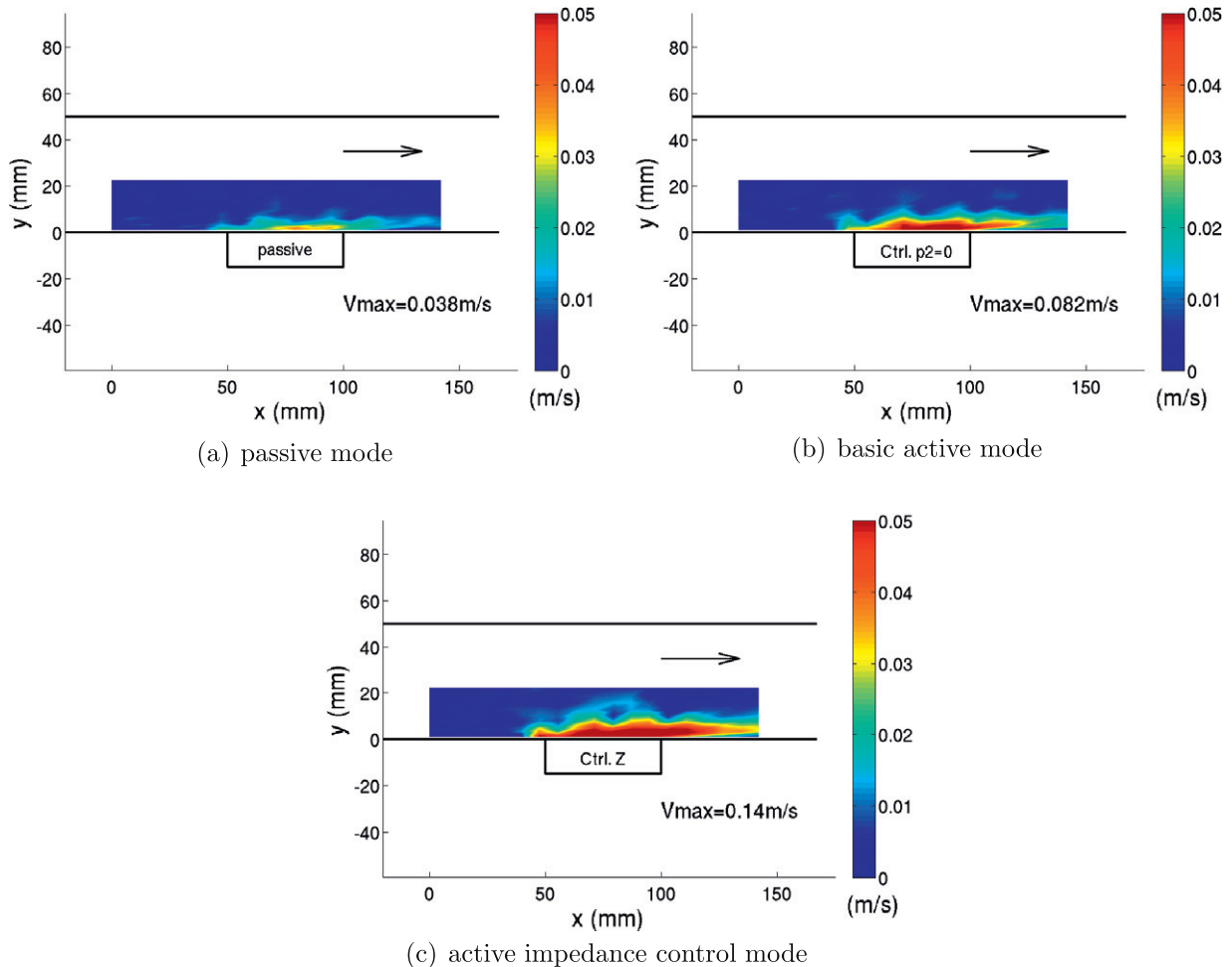


Fig. 13. Acoustic velocity in y -direction at 496 Hz, complex hybrid cell, $M = 0.1$.

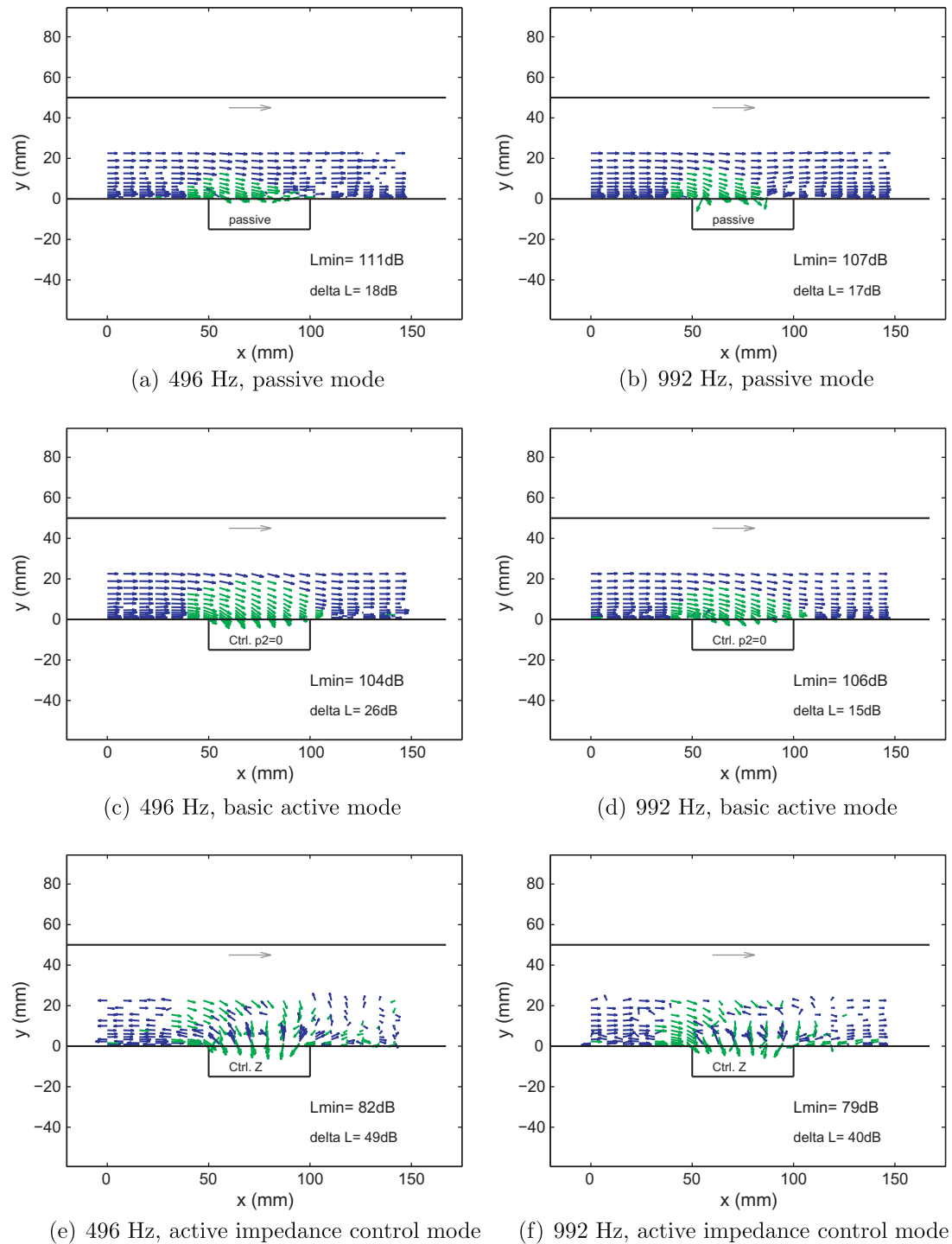


Fig. 14. Acoustic intensity, complex hybrid cell, $M = 0$.

Results without flow are showed in Fig. 9. In passive mode, normal velocity is small for both resistive screens. The screen of smaller resistance (the feltmetal sheet, Fig. 9a) results in slightly higher velocity than the screen of higher resistance (the wiremesh, Fig. 9c). Splices between the cells can be recognized, regions of non-zero normal velocity are limited to the vicinity of the three cells. Basic active control seems to enhance normal velocity,³ espe-

cially in the case of the feltmetal sheet (Fig. 9b). Considering Fig. 4a, we notice that this is indeed the layer producing an impedance closer to the predicted optimal impedance. The colorscale has been chosen to a range from 0 to 0.1 m/s, maximum values in Fig. 9b reach about 0.2 m/s though. The third cell is fairly inactive; it appears as if most of the sound power was absorbed before reaching the last cell. Fig. 9d is disturbed in vicinity of the third cell. In fact, the incense smoke did not sufficiently reach this region and measurements are inaccurate. To sum up, one observes a quite global influence on the duct in basic active mode and the splices between the three hybrid cells become invisible. The choice of the resistance

³ Primary excitation remains unchanged in respect to the passive case and the measured velocity in x direction is very similar.

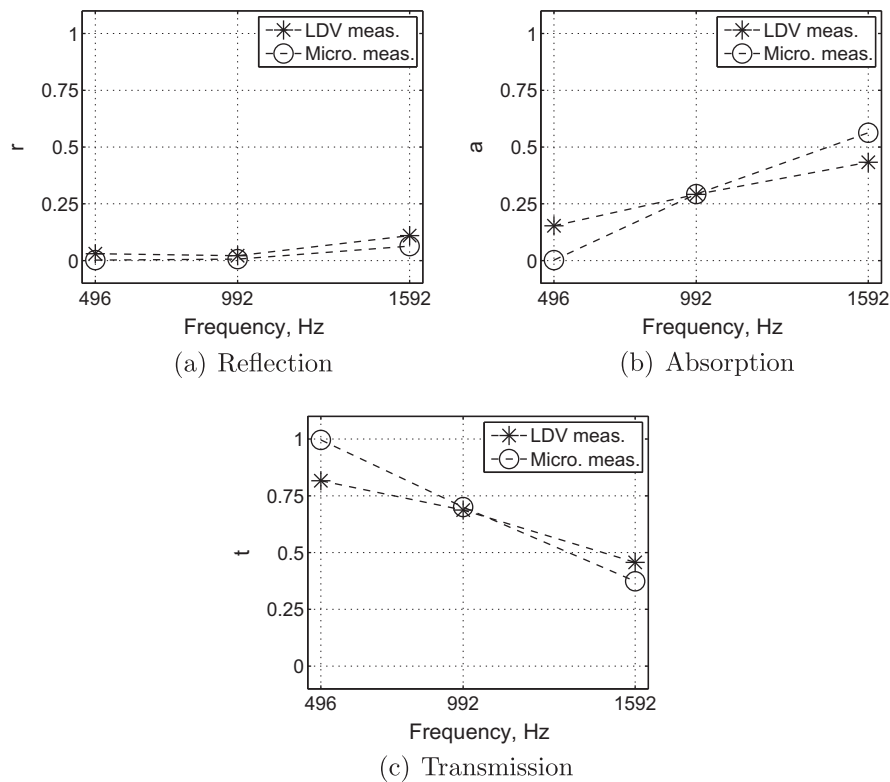


Fig. 15. Reflection, absorption, and transmission coefficients measured in the ONERA duct for the complex hybrid absorber in passive mode, $M = 0$.

of the resistive sheet has an important influence on the liner performance.

Let us now consider the situation with flow depicted in Fig. 10. In passive mode, the situation appears rather similar to the no flow case, however, due to the flow the colormap is less regular. In basic active mode, normal velocity is increased for both materials but zones of high normal velocity remain close to the three cells. This influence on the duct is less global than without flow. This is consistent with the experimental observation that transmission loss decreases in presence of flow. By contrast, the numerical calculation does not predict any significant drop of TL (see discussion in Section 3 about results of Fig. 5). Apparently, more realistic flow profiles had to be taken into account to predict these phenomena.

It has been mentioned that the amplification of acoustic velocity normal to the absorber enhances absorption. However, the presented figures do not visualize the energy flow. In order to clarify the influence of the absorber on the duct, intensity fields obtained with the feltmetal screen are given in Fig. 11. Intensity vectors whose continuation would impact the absorber are traced in green color, the others are in blue,⁴ and in all cases lengths are proportional to the intensity level. Evidently, acoustic power downstream the absorber has decreased in respect to the incident power. In agreement with the velocity measurements presented above, absorption is less pronounced in presence of flow. As brought up before (see Section 4.2), determination of intensity requires the estimation of acoustic pressure from the acoustic displacement field. This estimation is subject to larger phase errors at low frequencies, therefore the intensity fields at 992 Hz are cleaner than those at 496 Hz. At both frequencies, the reduced influence of the absorber in presence of flow can be observed.

5.2. The complex hybrid absorber

The complex hybrid absorber has been tested in three different modes of operation, i.e. passive mode, basic active mode (pressure cancellation $p_2 = 0$), and active impedance control mode. Corresponding surface impedances are summed-up in Table 2. As before, the analysis concentrates on the normal velocity component v_y at 496 Hz in a first time. Results are given in Fig. 12 for the no-flow case. Primary excitation is slightly lower in active impedance control mode than in passive mode and basic active mode. The basic active mode yields the expected result, i.e. an increase of velocity in respect to the passive mode. Keeping in mind the reduction of primary excitation in the active impedance control mode, the increase of normal velocity in this case is even larger than in the basic active mode. In presence of grazing flow, the influence of the absorber is again clearly reduced, as shown in Fig. 13. Active impedance control results in a slightly extended region of influence.

In contrast to the velocity measurements, the visualization of intensity in Fig. 14 reveals the difference between basic active mode (pressure cancellation) and active impedance control mode, without grazing flow and at 496 Hz and 992 Hz. Most intensity vectors point towards the impedance controlled absorber and the resulting downstream intensity amplitude is clearly reduced. Intensity charts in the grazing flow case are not available. Indeed, as mentioned in Section 4.1, the primary excitation had to be decreased due to saturation of the error microphones. Even though acoustic velocities that are significantly lower than the mean flow velocity can be measured, the primary excitation turned out to be too low to perform a proper calculation of acoustic pressure and acoustic intensity here.

Finally, LDV results and microphonic measurements are compared in terms of reflection (r), transmission (t), and absorption coefficients (a), defined in the following equations:

⁴ For interpretation of color in Figs. 3–5 and 7–14, the reader is referred to the web version of this article.

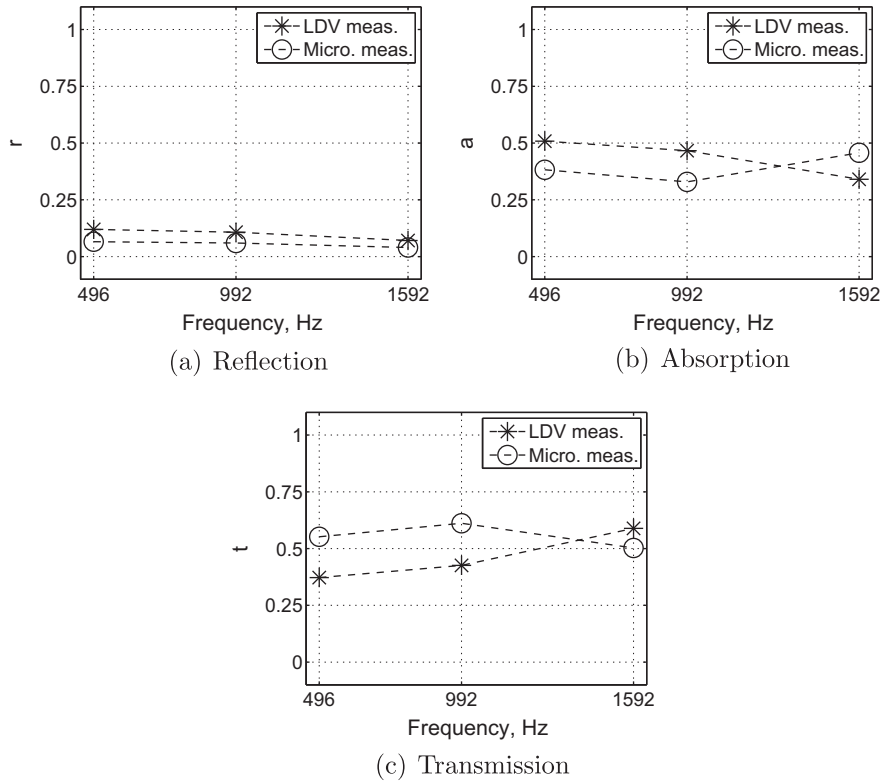


Fig. 16. Reflection, absorption, and transmission coefficients measured in the ONERA duct for the complex hybrid absorber in basic active mode ($p_2 = 0$), $M = 0$.

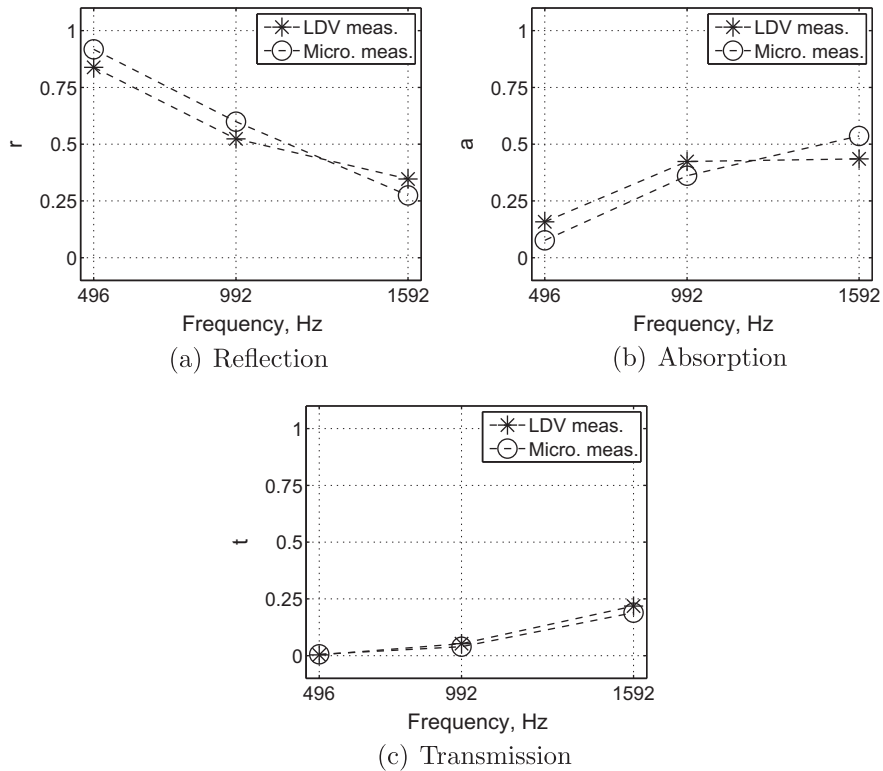


Fig. 17. Reflection, absorption, and transmission coefficients measured in the ONERA duct for the complex hybrid absorber in active impedance control mode, $M = 0$.

$$r = \frac{|A_R|}{|A_I|}^2 \quad (12)$$

$$t = \frac{|A_T|}{|A_I|}^2 \quad (13)$$

$$a = 1 - r - t \quad (14)$$

As we consider energetic coefficients, absorption can directly be deduced from reflection and transmission. The determination of these coefficients requires the detection of incident wave amplitudes A_I and reflected wave amplitudes A_R upstream the absorber using two microphones. Thanks to the anechoic outlet, the transmitted wave amplitude A_T is identified by a single microphone. Microphone measurements are performed upstream (at $x = -102$ mm, $x = -130$ mm or $x = -187$ mm) and downstream of the liner border (at $x = 252$ mm), and the spacing between the two upstream microphones is chosen to be part of the $[0.1\lambda/2, 0.8\lambda/2]$ interval given by Boden and Abom [27].

Reflection and transmission coefficients can also be obtained using the LDV measurements, provided a zone upstream and downstream the absorber is scanned. This is the case for the complex hybrid cell which only occupies 50 mm in the center of the measurement zone. For a reliable measurement, the distance between the upstream points has to be long enough. At the same time, we need to be as far as possible from the absorber in order to minimize the effect of evanescent waves. Two sections at $x = 0$ mm and $x = 32$ mm are chosen in order to perform the separation of upstream and downstream running waves. The transmitted wave is detected at $x = 142$ mm. The obtained reflection and transmission coefficients are quite constant in y -direction, i.e. waves are reasonably plane at the chosen distances. This is not the case for measurements closer to the absorber. The reflection and transmission coefficients obtained at different heights y are finally averaged and the associated absorption coefficient is computed. These values are summed up in Figs. 15–17 for the three modes of the hybrid cell (passive, basic control and active impedance control). Agreement between microphone measurements and LDV measurements is globally satisfying, even if LDV measurements are likely to be affected by evanescent waves. We observe that the basic active mode clearly increases absorption, while reflection remains small. On contrary, the active impedance control mode mainly increases reflection, especially at low frequencies. The absorption is in the same order of magnitude as in the basic active mode. Consequently, the transmission is greatly reduced in the active impedance control mode, which was expected since settings of this control mode were determined by maximizing TL.

6. Conclusion

Two kinds of hybrid active–passive liners have been developed at the LMFA. The basic hybrid absorber is made of a resistive screen backed by a cavity containing an acoustic source, which allows to mimic a 1/4-wavelength resonator by cancelling the pressure at the back of the screen. Consequently the impedance of the basic hybrid absorber can be considered as purely real and equal to the resistance of the resistive screen. The second liner, denoted as complex hybrid absorber, uses a more elaborated control strategy since it is directly the surface impedance of the liner that is fixed to a target value, with the help of two error microphones placed on each side of the resistive screen. However, when subject to grazing flow in the direction of sound propagation, these hybrid absorbers suffer from a loss of performance in respect to the no-flow case. Consequently, the local sound field around these liners has been investigated by means of non-intrusive LDV measurements, in order to throw some light on the origin of this change of efficiency.

Without flow, active control allows the velocity normal to the liner to be increased in a quite global way. This means that the different cells of the hybrid absorber cannot be distinguished anymore. The liner appears as a homogeneous and locally reacting liner. In the presence of grazing flow, this is not the case anymore. Normal velocity is only increased in the vicinity of the cells. The splices separating the cells of the liner become visible again, the influence on the duct remains local and absorption remains small.

The complex hybrid liner shows exceptional performance without flow. The tested (very short) absorber operates much like a reactive silencer, however, the absorber can also be tuned in a way to maximize absorption. In the presence of flow, the absorber behaves similarly as the basic hybrid absorber. In fact, the loss of performance seems to be global, i.e. not only due to the variation of optimal impedance induced by the presence of the flow. In this sense, a finer calculation of optimal impedance, taking into account the splices and more realistic flow profiles, should be done. The performed measurements are a basis for the validation of such a code.

Concerning future tests, the complex hybrid absorber will have to be equipped with microphones that support higher SPL, to get rid from saturation issues observed in the present LDV campaign. Moreover, a more compact absorber could be designed, for instance by replacing loudspeakers by piezo-actuators. However, this would not be immediate, since piezo-actuators usually work in a thinner frequency range than loudspeakers. The control strategy could also be slightly changed. Indeed, from now on, the passive resistance of the resistive layer is used as a predetermine input in the control loop (see Eq. (4)), and has to be measured in a standing wave tube without flow. However, depending on the choice of resistive sheet, the change in impedance because of the presence of grazing flow cannot always be neglected. So, the performance of complex hybrid liner could be improved by measuring this resistance, before active control, thanks to the standard “two-microphones” technique [28] with pressure signals p_1 and p_2 . The reactance could also be introduced in the cost function. Measurements in the presence of flow opposite to sound propagation would also represent an interesting completion, insofar as the performance of the liner is likely to be enhanced compared to the no flow case.

Compared to a classical ANC algorithm, based on an “anti-noise” concept, imposing a “target” impedance appears more stable and robust. The coherency between actuator and sensors signals is naturally high due to their closeness. As less voltage is required for the actuator, its saturation and the associated non-linear effects are less likely to happen. Then, there is no parasite feedback effect on the reference sensor that could prevent the adaptive algorithm from converging. Moreover, in cases where many acoustic modes can propagate within the duct, the impedance control does not require any knowledge of a modal model to ensure the correct position of the error sensor and does not produce any phenomena of spillover if modal coupling arises.

Finally for industrial applications, as the impedance is intrinsic to the liner, a target value can be chosen by the manufacturer and, so on, satisfied by the active control process without taking into account the global environment. However, the assumption of localized reaction of the active liner that is used in the present control strategy (i.e. the impedance of the hybrid liner is assumed to be independent of the acoustic waves incidence) requires that the width of the liner is small compared to the noise wavelength. Thus, reducing the sound field of high order modes in a turboengine nacelle with the whole section covered by elementary hybrid absorbers is obviously not realistic. Nevertheless, controlling the impedance on a limited surface can have a significant effect on the global radiated pressure field. Numerical computations with CAA solvers could help to optimize the surface of treatment.

References

- [1] Jones M, Tracy M, Watson W, Parrott T. Effects of liner geometry on acoustic impedance. In: 8th AIAA/CEAS conference, Breckenridge, Colorado, USA, 2002 [AIAA 2002-2446].
- [2] Dupont J-B, Galland M-A. Active absorption to reduce the noise transmitted out of an enclosure. *Appl Acoust* 2009;70(1):142–52.
- [3] Mazeaud B, Galland M-A, Sellen N. Design of an adaptive hybrid liner for flow duct applications. In: 10th AIAA/CEAS aeroacoustics conference, Manchester, Great Britain, 2004 [AIAA-2004-2852].
- [4] Galland M-A, Sellen N, Cuesta M. Noise reduction in a flow duct: Implementation of a hybrid passive/active solution. *J Sound Vib* 2006;297:492–511.
- [5] Olson H, May E. Electronic sound absorber. *J Acoust Soc Am* 1953;25(6):1130–6.
- [6] Kanev N, Mironov M. Active resonators for sound control in narrow pipes. *Acoust Phys* 2008;54(3):437–43.
- [7] Lissek H, Boulandet R, Fleury R. Electroacoustic absorbers: bridging the gap between shunt loudspeakers and active sound absorption. *J Acoust Soc Am* 2011;129(5):2968–78.
- [8] Betgen B, Galland M-A. A new hybrid active/passive sound absorber with variable surface impedance. *Mech Syst Sig Process* 2011;25(11):1715–26.
- [9] Galland M-A, Mazeaud B, Sellen N. Hybrid passive/active absorbers for flow ducts. *Appl Acoust* 2005;66(6):691–708.
- [10] Betgen B, Galland M-A, Piot E, Simon F. Characterization of a hybrid active-passive liner by means of Laser Doppler Velocimetry. In: 16th AIAA/CEAS aeroacoustics conference, Stockholm, Sweden, 2010 [AIAA-2010-3808].
- [11] Mazeaud B, Galland M-A. A multi-channel feedback algorithm for the development of active liners to reduce noise in flow duct applications. *Mech Syst Sig Process* 2007;21(7):2880–99.
- [12] Cremer L. Theorie der Luftschall-Dämpfung im Rechteckkanal mit schluckender Wand und das sich dabei ergebende höchste Dämpfungsmass. *Acustica* 1953;3:249–63.
- [13] Tester B. The propagation and attenuation of sound in lined ducts containing uniform or “plug” flow. *J Sound Vib* 1973;28(2):151–203.
- [14] Elnady T, Boden H. An inverse analytical method for extracting liner impedance from pressure measurements. In: 10th AIAA/CEAS aeroacoustics conference, Manchester, Great Britain, 2004 [AIAA-2004-2836].
- [15] Auregan Y, Leroux M, Pagneux V. Measurement of liner impedance with flow by an inverse method. In: 10th AIAA/CEAS aeroacoustics conference, Manchester, Great Britain, 2004 [AIAA-2004-2838].
- [16] Jing X, Peng S, Sun X. A straightforward method for wall impedance reduction in a flow duct. *J Acoust Soc Am* 1953;124(1):227–34.
- [17] Rienstra S. A classification of duct modes based on surface waves. *Wave Mot* 2003;37:119–35.
- [18] Myers M. On the acoustic boundary condition in the presence of flow. *J Sound Vib* 1980;71(3):429–34.
- [19] Betgen B. Comportement d'un absorbant actif en coulement: tude thorique et experimentale, Ph.D. thesis, Ecole Centrale de Lyon; 2010.
- [20] Minotti A, Simon F, Ganti F. Characterization of an acoustic liner by means of Laser Doppler Velocimetry in a subsonic flow. *Aerospace Sci Technol* 2008;12(5):398–407.
- [21] Chung JY. Rejection of flow noise using a coherence function method. *J Acoust Soc Am* 1980;62(2):388–95.
- [22] Nance D, Ahuja KK. Limitations of the three-microphone signal enhancement technique. In: 45th AIAA aerospace sciences conference, Reno, NV, 2007 [AIAA 2007-441].
- [23] Minotti A, Simon F, Piet JF, Millan P. Signal processing for in-flow measurement of acoustic velocity by LDV. In: 8th AIAA/CEAS aeroacoustic conference & exhibit, Breckenridge, Colorado, 2002.
- [24] Lavielle M, Simon F, Micheli F. Measurement of acoustic quantity fields in duct flow by Laser Doppler Velocimetry. In 12th AIAA/CEAS aeroacoustics conference, Cambridge, Massachusetts; 2006 [AIAA 2006-2550].
- [25] Brazier JP. Derivation of an exact energy balance for Galbrun equation in linear acoustics. *J Sound Vib* 2011;330(12):2848–68.
- [26] Cantrell R, Hart R. Interaction between sound and flow in acoustic cavities: mass, momentum and energy considerations. *J Acoust Soc Am* 1964;36(4):697–706.
- [27] Boden H, Abom M. Influence of errors on the two microphones method for measuring acoustics properties in ducts. *J Acoust Soc Am* 1986;79(2):541–9.
- [28] Dean P. An in situ method of wall acoustic impedance measurement in flow ducts. *J Sound Vib* 1974;34(1):97–130.